A Simple Method For Separating Weak And Strong Moving Targets In Clutter For A Radar System Using The Fractional Fourier Transform

Seema Sud *seema.sud@aero.org*
Communications and Signal Analysis Department
The Aerospace Corporation
Chantilly, VA 20151, USA

Abstract

The Fractional Fourier Transform (FrFT) is a powerful tool that utilizes the time-frequency plane to separate signals-of-interest (SOIs) from interference and noise in non-stationary environments. This requires estimation of the rotational parameter 'a', which is typically chosen as the value that minimizes the mean-square error between the desired SOI and its estimate or that minimizes the overlap of the projection of the signal and noise onto the axis 't_a'. The FrFT has successfully been used in many applications, but it is most suited for applications in which the time and frequency content of an SOI and the undesired interference are different, and it has been shown to greatly outperform the conventional Fast Fourier Transform (FFT). In this paper, we develop a simple algorithm that applies the FrFT to separate multiple moving targets in a radar system from each other, as well as from the clutter filled environment. The algorithm utilizes the fact that echoes from moving targets are chirps, and therefore project onto the optimum rotational axis in the FrFT domain just as a single CW tone projects in the FFT domain. By searching for peaks and notching them out, we can remove high power moving targets, enabling us to extract low power ones. This algorithm is robust in clutter because clutter does not correlate with the chirp signal in the FrFT domain, and thus does not impair our ability to estimate the chirp signal peaks. We show that the performance of the proposed algorithm is robust using up to three simultaneous moving targets in clutter for signal-to-clutter ratios (SCRs) of SCR = 0 and 10 dB when the weakest target is 8 and 20 dB below the strongest one, respectively.

Keywords: Chirp, Clutter, Fractional Fourier Transform, Radar.

1. INTRODUCTION

The Fractional Fourier Transform (FrFT) has been applied to problems in fields such as quantum mechanics, optics [1], image processing, data compression, and signal processing for communications ([2] and [3]). The FrFT is a very useful tool for separating a signal-of-interest (SOI) from interference in a non-stationary environment [3]. The problem of separating multiple moving targets of differing power levels received by a monostatic radar system in clutter lends itself nicely to implementation by the FrFT because moving target echoes are chirp signals, which can be easily separated in the FrFT domain. We propose an algorithm that is much simpler to implement than a previous algorithm, which relied on computing peak to sidelobe ratios (PSRs) in the FrFT domain to estimate the chirps [4]. The algorithm differs from that presented in [5], which uses the FrFT to extract both stationary and moving targets assuming that they have high signal-to-clutter ratios (SCRs) and high signal-to-noise ratios (SNRs) by using matched filtering and correlation methods. The simpler problem of extracting a single target in clutter using time delay correlation methods is presented in [6] and using clutter map cancellation in [7]. Extracting a single weak target in clutter by performing clutter subtraction is given in [8]. Finally, multiple strong targets are separated with the FrFT using multiple channels in a bi-static SAR in [9] and in [10].

In this paper, we propose to use the FrFT to extract multiple targets in clutter, where some targets are very weak. To do this we first remove strong targets by rotating to the proper axis 't_a' using rotational parameter 'a', in which the target chirp becomes a strong tone. By simply searching for the maximum peak over all values of 'a', we easily find and notch out strong moving target echoes, and can therefore pull out the weaker ones.

The paper outline is as follows: Section 2 briefly reviews the FrFT and its relation to the Wigner Distribution, which is a useful visual tool for understanding the FrFT. Section 3 describes the signal model and conventional echo detection for weak target detection as described in [4]. Section 4 discusses the proposed detection algorithm using the FrFT. Section 5 has simulation results showing the robust performance of the proposed FrFT method. Conclusions and remarks on future work are given in Section 6.

2. BACKGROUND: FRACTIONAL FOURIER TRANSFORM (FrFT)

The FrFT of a function f(x) of order 'a' is defined as [3]

$$\mathbf{F}^a[f(x)] = \int_{-\infty}^{\infty} B_a(x,x')f(x')dx', \tag{1}$$

where the kernel $B_a(x,x')$ is defined as

$$B_a(x,x') = \frac{e^{i(\pi\hat{\phi}/4-\phi/2)}}{|sin\phi|^{1/2}} \times e^{i\pi(x^2cot\phi - 2xx'csc\phi + x'^2cot\phi)}, \tag{2}$$

$\phi = a\pi/2$, and $\hat{\phi} = sgn[sin(\phi)]$. This applies to the range $0 < |\phi| < \pi$, or $0 < |a| < 2$. In discrete time, we can model the N × 1 FrFT of an N × 1 vector **x** as

$$\mathbf{X}_a = \mathbf{F}^a\mathbf{x}, \tag{3}$$

where $\mathbf{F}^a$ is an N × N matrix whose elements are given by ([11] and [3])

$$\mathbf{F}^a[m,n] = \sum_{k=0,k\neq(N-1+(N)_2)}^{N} u_k[m]e^{-j\frac{\pi}{2}ka}u_k[n], \tag{4}$$

and where $u_k[m]$ and $u_k[n]$ are the eigenvectors of the matrix **S** defined by [11]

$$\mathbf{S} = \begin{bmatrix} C_0 & 1 & 0 & \dots & 1 \\ 1 & C_1 & 1 & \dots & 0 \\ 0 & 1 & C_2 & \dots & 0 \\ \vdots & \vdots & \vdots & \ddots & \vdots \\ 1 & 0 & 0 & \dots & C_{N-1} \end{bmatrix}, \tag{5}$$

and

$$C_n = 2cos(\frac{2\pi}{N}n) - 4. \tag{6}$$

Numerous methods are presented in the literature for implementing the FrFT efficiently (see for example [12] and [11]).

The Wigner Distribution (WD) is a time-frequency representation of a signal, and may be viewed as a generalization of the Fourier Transform, which is solely the frequency representation. The WD of a signal x(t) can be written as

$$W_x(t,f) = \int_{-\infty}^{\infty} x(t+\tau/2)x^*(t-\tau/2)e^{-2\pi j\tau f}d\tau. \tag{7}$$

It is well-known that the projection of the WD of a signal x(t) onto an axis t_a gives the energy of the signal in the FrFT domain 'a', $|\mathbf{X}^a(t)|^2$ (see e.g. [2] or [13]). Letting α = aπ/2, this is written as

$$|\mathbf{X}_\alpha(t)|^2 = \int_{-\infty}^{\infty} W_x(tcos(\alpha) - fsin(\alpha), tsin(\alpha) + fcos(\alpha))df. \tag{8}$$

In discrete time, the WD of a signal x[n] is written as [14]

$$W_x[\frac{n}{2f_s}, \frac{kf_s}{2N}] = e^{j\frac{\pi}{N}kn} \sum_{m=l_1}^{l_2} x[m]x^*[n-m]e^{j\frac{2\pi}{N}km}, \tag{9}$$

where l_1 = max(0,n−(N-1)) and l_2 = min(n,N −1). This particular implementation of the discrete WD is valid for non-periodic signals. Aliasing is avoided by oversampling the signal x[n] using a sampling rate of fs [samples per second] that is at least twice the Nyquist rate [14].

Radar echoes from moving targets are chirp signals, and we show the WD of a chirp signal x(t) in Fig. 1. The figure illustrates how the FrFT may be used to detect chirp signals. If we rotate to the axis 't_a' and compute the energy in the FrFT, the chirp projects onto the axis as a strong tone, which can be detected and notched by finding the peak of the energy, using Eq. (8). Then lower power chirps, at other rotational axes, can be detected by repeating the process.

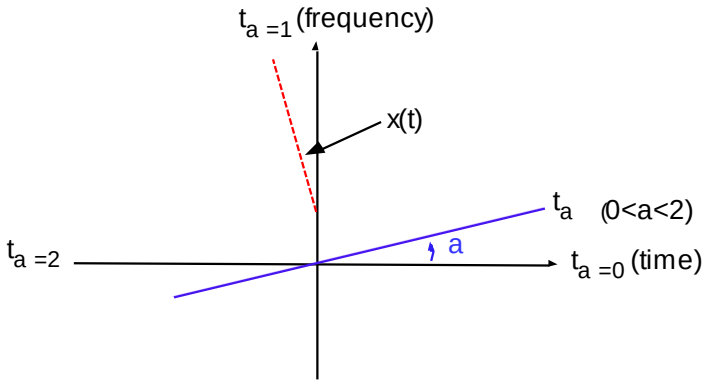

FIGURE 1: Wigner Distribution of chirp signal x(t).

3. SIGNAL MODEL AND CONVENTIONAL TARGET DETECTION WITH FrFT

We follow the signal model presented in [4]. Assume that there is an airborne radar platform such as a plane moving along the y-axis at constant speed V and a moving target i at an initial distance $R_{0,i}$ away, at time t = 0, moving with speed v_i and acceleration a_i, potentially in a different direction as the plane (see Fig. 2). After a time t the platform and target have moved a total distance of Vt and $v_i t + \frac{1}{2}a_i t^2$, respectively. The components of the speed of the target along the x- and y-axes are $v_{r,i}$ and $v_{c,i}$, and similarly $a_{r,i}$ and $a_{c,i}$ for the acceleration. At time t, target i is now at a distance

from the platform whose horizontal component has decreased by $v_{r,i}t + \frac{1}{2}a_{r,i}t^2$ and likewise the vertical component has decreased by $v_{c,i}t + \frac{1}{2}a_{c,i}t^2$. Accordingly, the distance between the target and radar can be approximated by [4]

$$R_i(t) \approx R_{0,i} - v_{r,i}t + [(V - v_{c,i})^2 - R_{0,i}a_{r,i}]\frac{t^2}{2R_{0,i}}. \tag{10}$$

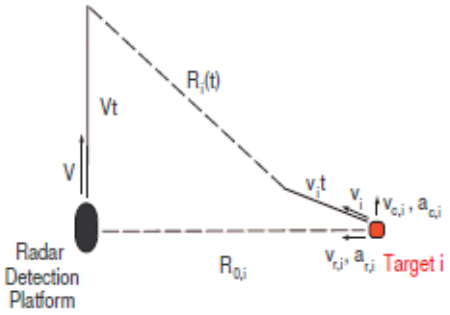

FIGURE 2: Radar detection platform and moving target scenario

As discussed in [4], the echo of the moving target as received by the radar system can be approximated by a chirp signal that takes the form

$$x_i(t) = e^{j2\pi f_{d,i}t}e^{j\pi K_i t^2}, \tag{11}$$

where

$$f_{d,i} = \frac{2v_{r,i}}{\lambda}, \tag{12}$$

$$K_i = \frac{2}{\lambda R_{0,i}}[-(V - v_{c,i})^2 + R_{0,i}a_{r,i}], \tag{13}$$

λ is the wavelength of the radar, related to its frequency f by λ = c/f, and c = 3×10^8 m/s is the speed of light. We further assume there are no strong point scatterers, so that the ground (i.e. surface) clutter may be adequately modeled as additive white Gaussian noise (AWGN), using a desired SCR. If we now assume a scenario with multiple moving targets, with K targets total, we can write the composite received echo signal as

$$x(t) = \sum_{i=1}^{K} A_i x_i(t) + n(t), \tag{14}$$

where n(t) is a combination of clutter and noise using a given SCR and each amplitude A_i is chosen to model strong and weak targets. If we assume, without loss of generality, that signal i = 1 is the main target, we can model the amplitudes A_i for i = 2, 3, ..., K using an assumed carrier-to-interference ratio (CIR) by writing $A_i = 10^{-CIR_i/20}$.

The algorithm given in [4] is based on the fact that a chirp signal in the FFT domain is spread out over a band of frequencies, whereas at the optimum rotational parameter 'a' (as shown in Fig. 1), the projection of the signal onto that axis, given by the magnitude squared of its FrFT, is maximized. This signal is therefore estimated by computing a peak and comparing it to the sidelobe level to determine a detection. It is then removed by applying a narrow, bandstop filter.

Next, by rotating back to the time domain, the operation is performed again to find the second strongest signal, the third strongest, etc.

4. PROPOSED ECHO SEPARATION METHOD USING FrFT[1]

The proposed algorithm modifies that in [4] with four simplifying calculations: (1) We compute the rotational parameter of the strongest signal, a_1, at which the energy of the Wigner Distribution is maximum by computing the peak of the FrFT at all angles and simply choosing the maximum. This avoids sidelobe computation at each 'a', which is unnecessary in an environment of moving targets in noise and clutter; (2) Once the value of a_1 is calculated, instead of computing a bandstop filter to remove the strong signal, we simply rotate to the axis a_1, in which the desired signal is now a tone, find the peak along this new rotational axis and set it to zero, thereby notching out the target to search for subsequent lower power targets. This also greatly simplifies the algorithm by avoiding the complexity of filtering; (3) Instead of performing two rotations to look for the next strongest signal, i.e. first to $-a_1$ and then to a_2, we simply rotate to $a_2 - a_1$, hence performing the next rotation in one step; (4) We only perform the FrFT at all angles 'a' once, since we can notch signals out and look for the next peak without another search.

We summarize the proposed algorithm in Table 1. We let the step size for a, Δa, be equal to 0.01 and collect N = 1,000 samples of the composite echo signal x(t). Note that once each signal is isolated, conventional signal processing can be performed to compute any desired parameters associated with the target.

Initialize: $a_{0,opt} = 0; \quad i = 1;$

1. For $a = 0 : \Delta a : 2$ % Loop over all a
   $\mathbf{X}(a) = \mathbf{F}^a x(t)$; % Compute FrFT of x(t), given in Eq. (14)
   $X_{max,i}(a) = max(|\mathbf{X}(a)|)$; % Compute max value
   End
2. $a_{i,opt} = \underset{a}{arg\ max}\ X_{max,i}(a)$; % Find peak over all a
3. $\mathbf{X}_{peak,i}(t_{a_{i,opt}}) = \mathbf{F}^{[a_{i,opt} - a_{i-1,opt}]} x(t)$; % Rotate to signal i
4. $X_{max,i}(a)|_{a_{i,opt}} = 0$; % Notch out peak i
5. $\mathbf{X}_{peak,i}(t_{a_{i,opt}})|_{max} = 0$; % Notch out signal i
6. $x_{i+1}(t) = \mathbf{F}^{-(a_{i,opt} - a_{i-1,opt})} \mathbf{X}_{peak,i}(t_{a_{i,opt}})$; % Rotate back to $a = 0$
7. Increment $i = i + 1$ and repeat Steps 2-5 for $i = 2, 3, ..., K$.
   (Step 6 is optional for plotting the intermediate time domain signal.)

TABLE 1: Proposed weak target extraction algorithm.

5. SIMULATIONS

We model the three targets given in [4], whose parameters are repeated for convenience in Table 2. In the first example, we assume that only targets 1 and 2 are present, with SCR = 10 dB, and CIR_2 = 6 dB. The results are shown in Fig. 3, where we plot $X_{max,i}$, $X_{peak,i}$, and FFT$\{x_{i+1}(t)\}$ from Steps 1, 3, and 6 in Table 1, dropping the indices for convenience. Note the good detection and signal removal performance. We also point out that a target whose optimum detection parameter is 'a' will still project energy onto an axis a ± Δe, where here Δe is about 0.01 − 0.02; we call this signal leakage. This means that we can only resolve signals that are separated by 0.025 in 'a' (note that the step size in [4] is not provided; a larger step size could be a cause of the need for a more complex algorithm). To reduce Δe requires a smaller Δa, at a processing cost in Step 1 of the proposed algorithm.

[1] Patent Pending

Target, i	$v_{r,i}[m/s]$	$v_{c,i}[m/s]$	$a_{r,i}[m/s^2]$
1	0.67	5	2.54
2	1.67	−5	3.97
3	2.33	3	1.03

TABLE 2: Parameters of simulated targets.

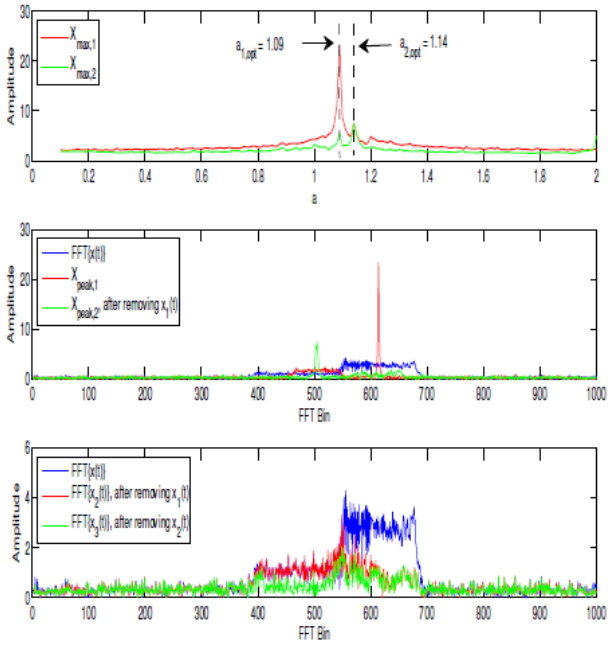

FIGURE 3: K = 2 Targets; SCR = 10 dB, CIR_2 = 6 dB

The second example in Fig. 4 shows two users where now the SCR has been reduced to 0 dB and CIR_2 has been increased to 8 dB, and the detection algorithm continues to perform well. Note from the first plot in the figure that notching out $x_1(t)$ still results in a small peak about $a_{1,opt}$ (from the signal leakage and noise). As CIR_2 continues to increase, i.e. signal $x_2(t)$ continues to get weaker compared to $x_1(t)$, then we may not be able to accurately estimate its rotational parameter because the small peak near $a_{1,opt}$ may dominate. If such a condition is expected to occur, we can

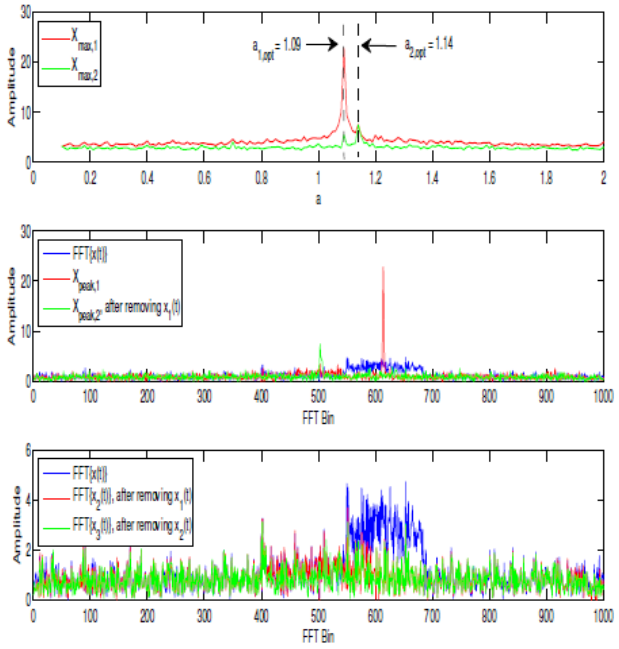

FIGURE 4: K = 2 Targets; SCR = 0 dB, CIR_2 = 8 dB

reduce Δa or slightly modify the proposed algorithm to null one or two samples about the peak at $a_{1,opt}$ to avoid the problem. Then, the algorithm will correctly select $a_{2,opt}$.

In the next example, we add the third target, using SCR = 0 dB, CIR_2 = 3 dB, and CIR_3 = 8 dB. The result is given in Fig. 5 where we see the detection is still achieved, and the last plot shows that performance of the algorithm notching out successive signals is as good as before, even for a third signal.

In the last example, we let SCR = 10 dB, CIR_2 = 5 dB, and CIR_3 = 20 dB. In this case, the simulation shows that using Δa = 0.01 is not sufficient to accurately estimate $a_{3,opt}$. So, we set Δa = 0.0001, with good results as shown in Fig. 6. Note from the third plot that because the signal is already so weak, that notching out the signal does not change the spectrum much, as is expected. From this example, we see that to detect weak signals, we can simply make Δa smaller. There is a limit, however, since if the signal becomes too weak, then it cannot be estimated in the clutter, no matter how small Δa is. Signals that are 20 dB below the strongest signal and 10 dB below the clutter are about the weakest that can be detected and notched by this algorithm. That is, if CIR_3 goes higher 20 dB or SCR goes lower than 10 dB, the algorithm may start to have errors in finding $a_{3,opt}$ and hence detecting and notching the third signal. This can be noted in the figure as the peak in the black curve in the first plot is just barely above the floor, and it would be obscured by higher clutter levels or if the signal were weaker. Further study is required to address this problem.

This algorithm provides significant improvement over that given in [4], which appears to assume the weak target is no more than 7-8 dB below the strong one, although this is not explicitly stated. Hence, this method can operate at 12-13 dB lower CIR and is a more computationally efficient algorithm since it does not require peak-to-sidelobe energy calculations. Prior techniques based on a combined Wigner Distribution (WD) and Radon Transform (RT) did not perform well in the presence of multiple targets, e.g. [15]. Other methods improve upon that in [15] but at the expense of loss of time or frequency resolution in signal separation.

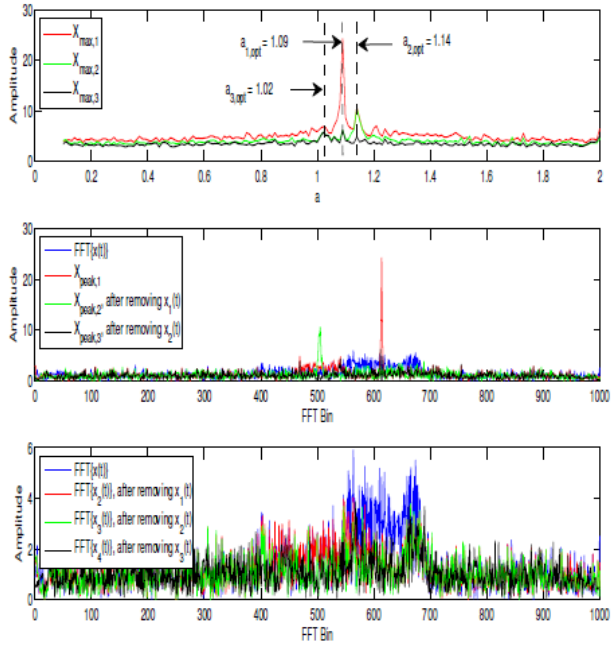

FIGURE 5: K = 3 Targets; SCR = 0 dB, CIR_2 = 3 dB, CIR_3 = 8 dB.

Two important points are as follows. First, we note that the proposed algorithm can also be applied when users have equal or near equal power. In this case, the users who appear to have slightly stronger power in $X_{max,i}$ will be notched first. Second, note that instead of notching strong users to look for weaker ones, we can extract the strong user for further processing. This can be done by notching everywhere except for the peak in step 4 above. That is, we set

$$X_{peak,i}(t_{ai,opt})|_{\neq \max} = 0, \tag{15}$$

where this notation indicates that we set all values except for the maximum value to zero. This new signal now contains the strong target and can be rotated back to the time domain just as in step 5 above.

6. CONCLUSION

In this paper, we present a simple, robust algorithm for extracting both strong and weak targets in a moving target environment with clutter. The algorithm applies the Fractional Fourier Transform (FrFT). Since target echoes are chirp signals, when rotated to the fractional domain 'a' that maximizes the energy in the FrFT (i.e. their projection onto the axis 't_a' in the Wigner Distribution), they become tones. Tones from stronger signals are notched out and the resultant signal is rotated again to notch out the next strongest signal. Hence, very weak signals in clutter can be extracted. We show the algorithm works in finding and notching users that are up to 20 dB below the strongest one and up to 10 dB below the clutter; if clutter power is the same as signal power, we show that we can still extract users that are 8 dB weaker. Future work includes determining how to pull out weak targets that are more than 20 dB weaker than a strong target and more than 10 dB weaker than the clutter. Evaluating performance of the algorithm with greater than three targets is also a potential area for further study.

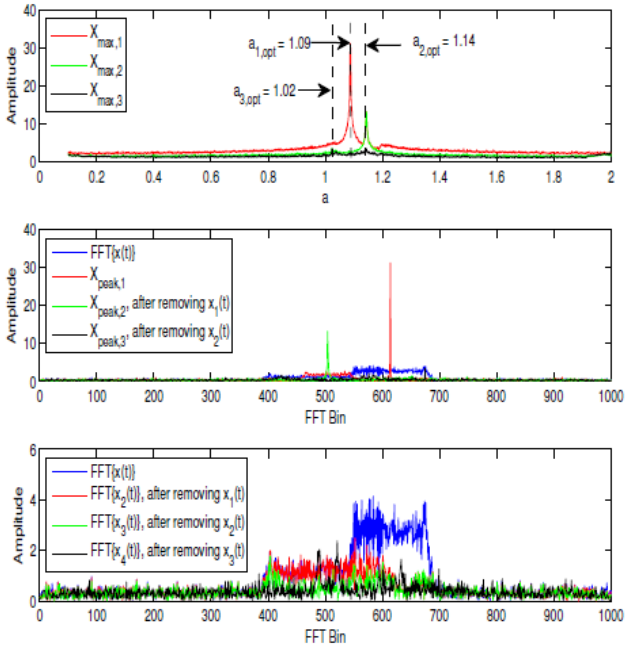

FIGURE 6: K = 3 Targets; SCR = 10 dB, CIR_2 = 5 dB, CIR_3 = 20 dB.

7. ACKNOWLEDGMENTS

The author gratefully acknowledges The Aerospace Corporation for funding this work and Alan Foonberg & Diana Johnson for reviewing the paper and providing helpful comments.

8. REFERENCES

[1] Bultheel, A., and Sulbaran, H.E.M., "Computation of the Fractional Fourier Transform", Int. Journal of Applied and Computational Harmonic Analysis 16 (2004), pp. 182-202.

[2] Kutay, M.A., Ozaktas, H.M., Arikan, O., and Onural, L., "Optimal Filtering in Fractional Fourier Domains", IEEE Trans. on Sig. Proc., Vol. 45, No. 5, May 1997.

[3] Ozaktas, H.M., Zalevsky, Z., and Kutay, M.A., "The Fractional Fourier Transform with Applications in Optics and Signal Processing", West Sussex, England, John Wiley and Sons, 2001.

[4] Sun, H.-B., Liu, G.-S., Gu, H., and Su, W.-M., 'Application of the Fractional Fourier Transform to Moving Target Detection in Airborne SAR', IEEE Trans. on Aerosp. and Electr. Systems, Vol. 38, No. 4, Oct. 2002.

[5] Liu, H., and Zhu, M., "Applying Fractional Fourier Transform to Radar Imaging of Moving Targets", Proc. IEEE Geoscience and Remote Sensing Symp. (IGARSS), Toulouse, France, Jul. 21-25, 2003.

[6] Guo, H.Y., and Guan, J., "Detection of moving target based on Fractional Fourier Transform in SAR clutter", Proc. IEEE Int. Conf. on Sig. Proc. (ICSP), Beijing, China, Oct. 24-28, 2010.

[7] Chen, X., Huang, Y., Guan, J., and He, Y., "Sea Clutter Suppression and Moving Target Detection Method Based on Clutter Map Cancellation in FRFT Domain", Proc. IEEE CIE Int. Conf. on Radar, Chengdu, China, Oct. 24-27, 2011, pp. 438-441.

[8] Deqiang, Y., and Haiyan, G., "Weak Target Detection Based on Fractional Spectral Subtraction in Sea Clutter", Proc. IEEE Int. Conf. on Electric Inform. and Control Eng. (ICEICE), Beijing, China, Apr. 15-17, 2011.

[9] Meng, Q., and Zhulin, Z., "A New Method of Moving Targets Detection and Imaging for Bistatic SAR", Proc. IEEE 7th Int. Symp. on Computational Intelligence and Design, Hangzhou, China, Dec. 13-14, 2014.

[10] Wu, J., Jiang, Y., Kuang, G., Lu, J., and Li, Z., 'Parameter Estimation for SAR Moving Target Detection Using Fractional Fourier Transform', IEEE Proc. IGARSS, Quebec City, QC, Canada, Jul. 13-18, 2014.

[11] Candan, C., Kutay, M.A., and Ozaktas, H.M., "The Discrete Fractional Fourier Transform", IEEE Trans. on Sig. Proc., Vol. 48, pp. 1329-1337, May 2000.

[12] Candan, C., Kutay, M.A., and Ozaktas, H.M., "The Discrete Fractional Fourier Transform", Proc Int. Conf. on Acoustics, Speech, and Sig. Proc. (ICASSP), Phoenix, AZ, Mar. 15-19, 1999, pp. 1713-1716.

[13] Kutay, M.A., Ozaktas, H.M., Onural, L., and Arikan, O. "Optimal Filtering in Fractional Fourier Domains", Proc. IEEE Int. Conf. on Acoustics, Speech, and Sig. Proc. (ICASSP), Vol. 2, 1995, pp. 937-940.

[14] O'Toole, J.M., Mesbah, M., and Boashash, B., "Discrete Time and Frequency Wigner-Ville Distribution: Properties and Implementation", Proc. Int. Symp. on Digital Sig. Proc. and Comm. Systems, Noosa Heads, Australia, Dec. 19-21, 2005.

[15] Barbarossa, S., "Analysis of Multicomponent LFM Signals by a Combined Wigner-Hough Transform", Proc. IEEE Trans. on Sig. Proc., 42, 1995, pp. 1511-1515.